

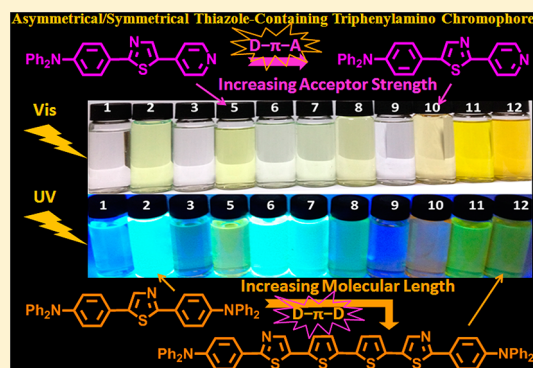
# Asymmetrical/Symmetrical D- $\pi$ -A/D- $\pi$ -D Thiazole-Containing Aromatic Heterocyclic Fluorescent Compounds Having the Same Triphenylamino Chromophores

Tao Tao, Bin-Bin Ma, Yu-Xin Peng, Xiao-Xu Wang, Wei Huang,\* and Xiao-Zeng You

State Key Laboratory of Coordination Chemistry, Nanjing National Laboratory of Microstructures, School of Chemistry and Chemical Engineering, Nanjing University, Nanjing 210093, People's Republic of China

## S Supporting Information

**ABSTRACT:** A family of linear asymmetrical D- $\pi$ -A and symmetrical D- $\pi$ -D types of thiazole-based aromatic heterocyclic fluorescent compounds bearing various electron-donating and electron-withdrawing tails (bromo, triphenylamino, pyridyl, thienyl and benzoic acid) have been designed and prepared successfully. Synthetic, structural, thermal, spectral and computational comparisons have been carried out for related compounds because of their adjustable electronic properties. It is interesting to mention that compound 2 can be prepared from 5-bromothiazole by one-pot Suzuki-Miyaura coupling and subsequent C-H activation reactions via a 5-TPA-substituted thiazole intermediate 1. X-ray single-crystal structures of six compounds indicate that they all crystallize in the triclinic  $P\bar{1}$  space group and the thiazole core exhibits different dihedral angles with its adjacent benzene ring of the triphenylamino group (3.6(3)–40.8(3) $^\circ$ ). The photophysical and electrochemical results demonstrate that compound 7 exhibits high electrochemical activity with a green fluorescence emission. Meanwhile, compounds 1, 2, and 6 show high luminescence quantum yields, and compound 8 exhibits excellent thermal stability ( $T_{d_{10}} = 503$   $^\circ\text{C}$ ).



## INTRODUCTION

Recently,  $\pi$ -functional materials<sup>1</sup> are of increasing interest on the studies of organic electronics, such as organic photovoltaics (OPVs), organic field-effect transistors (OFETs), and organic light-emitting diodes (OLEDs). For instance, many scientific efforts have been made on the extended aromatic heterocyclic systems, such as benzothiadiazole,<sup>2</sup> thiophene,<sup>3</sup> carbazole,<sup>4</sup> diazine,<sup>5</sup> naphthalene diimide,<sup>6</sup> perylene diimide,<sup>7</sup> and 1,10-phenanthroline,<sup>8</sup> which could act as effective components for the molecule-based photovoltaic and optoelectronic nano-devices. Furthermore, all these investigations present both opportunities and challenges to the rational design and synthesis of conjugated heterocyclic aromatic units for the applications of high-performance optoelectronic materials.

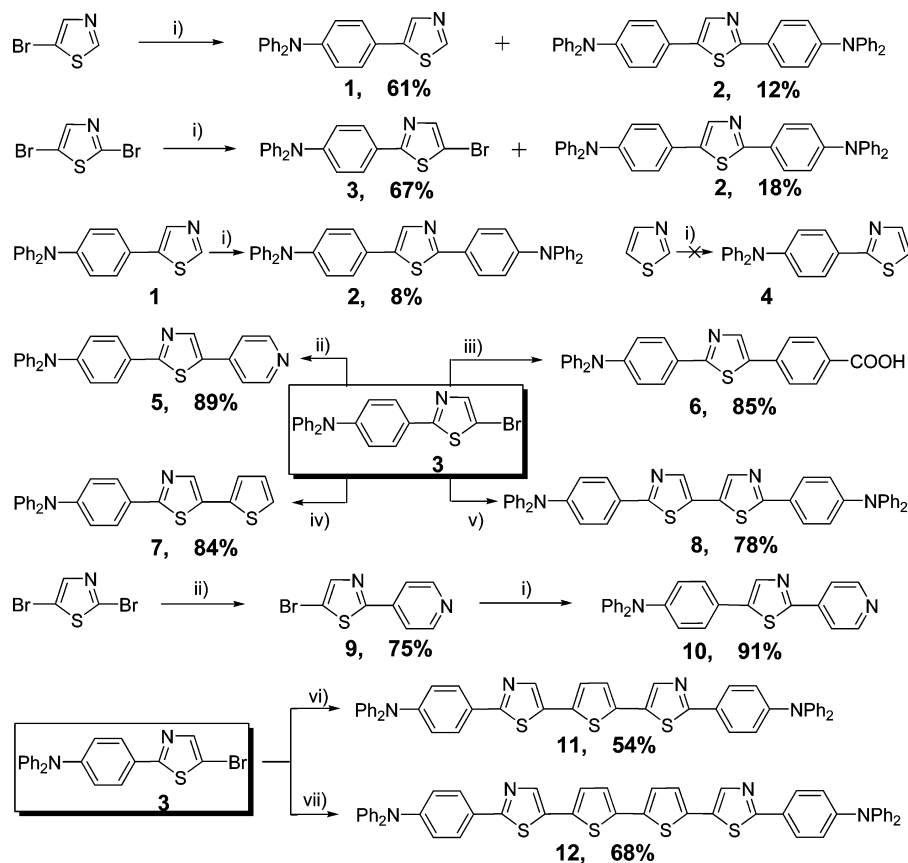
In view of the molecular design, one important problem is the fine-tuning of the electronic structures in a wide range and the precise control of the solid-state structures to achieve appropriate intermolecular interactions for bulk materials.<sup>9</sup> On the basis of the above-mentioned two considerations, it is believed that the linear thiophene/thiazole-containing conjugated compounds with different D-A hybrids are good candidates, and they represent an intriguing and promising class of  $\pi$ -conjugated oligomers. For example, Wakamiya and co-workers have demonstrated that the  $\text{B}(\text{C}_6\text{F}_5)_3$  coordination/cyclization protocol can be effective for tuning the electronic

structures of thiazolyl-capped conjugated skeletons.<sup>10</sup> Furthermore, different from macromolecules, organic small molecules are excellent model compounds and they show the better crystalline characteristics. X-ray single-crystal diffraction, which is widely regarded as a bridge between the theory and the experiment, has been proved to be one of the most powerful tools to characterize the molecular geometry and packing information.<sup>11</sup>

In our previous work, a series of symmetrical 1,10-phenanthroline, oligothiophene, and bithiazole-centered heterocyclic aromatic compounds and their photoresponsive self-assembled nanocomposite films and nanodevices have been investigated.<sup>12</sup> As an extensive study in this area, we aim to reduce the symmetry of our target molecules by using one asymmetrical thiazole core with different electron-donating and electron-withdrawing terminal groups. Generally, compounds with lower symmetry show fascinating properties, such as ferroelectric, near-infrared absorption, nonlinear optic, electro-generated chemiluminescence, single-molecular magnet, and asymmetrical catalysis.<sup>13</sup> The motivation of incorporating various donor and acceptor units into one molecule is to finely tune their electronic structures and compare their spectro-

Received: June 28, 2013

Published: August 13, 2013

Scheme 1. Synthetic Route of Thiazole-Containing Triphenylamino Compounds<sup>a</sup>

<sup>a</sup>(i) 4-(diphenylamino)phenylboronic acid, [Pd(PPh<sub>3</sub>)<sub>4</sub>], Cs<sub>2</sub>CO<sub>3</sub>, dioxane, H<sub>2</sub>O; (ii) 4-pyridinylboronic acid, [Pd(PPh<sub>3</sub>)<sub>4</sub>], Cs<sub>2</sub>CO<sub>3</sub>, toluene, H<sub>2</sub>O; (iii) 4-boronobenzoic acid, [Pd(PPh<sub>3</sub>)<sub>4</sub>], Cs<sub>2</sub>CO<sub>3</sub>, toluene, H<sub>2</sub>O; (iv) 2-thiophenylboronic acid, [Pd(PPh<sub>3</sub>)<sub>4</sub>], Cs<sub>2</sub>CO<sub>3</sub>, dioxane, H<sub>2</sub>O; (v) bis(pinacolato)diboron, [Pd(PPh<sub>3</sub>)<sub>4</sub>], KOH, dioxane, H<sub>2</sub>O; (vi) 2,5-bis(trimethylstannyl)thiophene, [Pd(PPh<sub>3</sub>)<sub>2</sub>Cl<sub>2</sub>], THF; (vii) 5,5'-bis(trimethylstannyl)-2,2'-bithiophene, [Pd(PPh<sub>3</sub>)<sub>2</sub>Cl<sub>2</sub>], THF.

scopic, electrochemical, and thermal properties. As a result, a family of symmetrical/asymmetrical thiazole-based heterocyclic aromatic fluorescent compounds with high thermal stability and good solubility has been described, where various electron-donating and electron-withdrawing terminal groups (bromo, triphenylamino, pyridyl, thienyl, and benzoic acid) are introduced, as illustrated in Scheme 1. Besides the conventional C–C coupling reactions, such as Suzuki–Miyaura, Stille, and homocoupling, the C–H activation reaction is achieved to prepare the unexpected TPA-functionalized thiazole compound **2** by the one-pot Suzuki–Miyaura coupling and the following C–H activation reactions via a 5-TPA-substituted thiazole intermediate **1**, and the possible reaction mechanism is proposed.

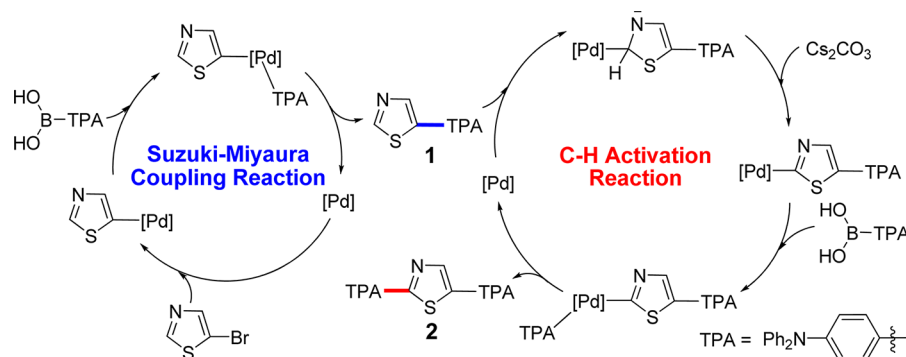
## RESULTS AND DISCUSSION

**Syntheses.** Thiazole is an asymmetrical molecule compared with thiophene, and the two  $\alpha$  positions of the sulfur atom have distinguishable reaction activities. However, the synthesis of asymmetrical thiazole-containing compounds remains more challenging than the symmetrical thiazole molecules.<sup>14</sup> Our synthetic strategy was based on the routes shown in Scheme 1, in which most of the thiazole-containing compounds were prepared by the Pd-catalyzed Suzuki–Miyaura and Stille cross-coupling reactions. The asymmetrical precursors **3** and **9** were synthesized from 2,5-dibromothiazole and respective boron reagents with high yields, where the 2-position of each thiazole

ring shows better reaction activity than its 5-position in the aspects of facilitating the C–C bond cross-coupling reactions and improving the final yields.<sup>15</sup> This difference in the reaction activity is successfully utilized to synthesize further asymmetrical thiazole-based compounds **5–7** and **10** with ease. Moreover, different from our previously reported bithiazole derivatives where the two TPA chromophores are introduced to 5- and 5'-positions of the central bithiazole unit,<sup>12g</sup> the C–C bond homocoupling reaction is first used to prepare **2** and 2'-TPA-substituted bithiazole compound **8** with a high yield (78%) in the presence of bis(pinacolato)diboron. All the heterocyclic aromatic compounds have been characterized by <sup>1</sup>H, <sup>13</sup>C NMR, and EI-TOF-MS spectra, and the results clearly demonstrate the formation of expected molecules. Furthermore, compounds **7**, **8**, **11**, and **12** have been confirmed by the <sup>1</sup>H–<sup>1</sup>H correlation spectroscopy (COSY) NMR, as illustrated in Figures SI6b, SI7b, SI10b, and SI11b (Supporting Information).

It is interesting to mention that the reaction between 1 equiv of 5-bromothiazole with 2 equiv of 4-(diphenylamino)phenylboronic acid under the conventional Suzuki–Miyaura coupling condition yields the expected compound **1** in a yield of 61%, as shown in Scheme 1. However, an unexpected byproduct **2** is also obtained simultaneously in a yield of 12%. This reaction can be monitored directly by a UV-light detector excited at 365 nm, in which the color of fluorescence emission alters from blue for the starting materials to yellow (**1**) and green (**2**). As a

Scheme 2. Possible Mechanism for the Formation of Unexpected Compound 2 Based on the One-Pot Suzuki–Miyaura Cross-Coupling and C–H Activation Reactions via a 5-TPA-Substituted Thiazole Intermediate 1



control experiment, thiazole was used to repeat the synthetic procedure instead of 5-bromothiazole, but no reaction took place and compound 4 was not found. The result indicates the low reactivity of C–H activation in this case, which is consistent with the previously reported literature.<sup>16</sup>

Taking all the above-mentioned results into consideration, it is concluded that at least two steps are required in this one-pot reaction. Namely, compound 1 was synthesized first by the classical Suzuki–Miyaura cross-coupling reaction, where the 5-TPA-substituted thiazole would activate the 2-position of the thiazole ring for the next reaction, and then compound 2 was generated from compound 1 by the normal Pd-catalyzed C–H activation reaction. A possible two-step reaction mechanism for producing compounds 1 and 2 is given in Scheme 2 to explain our experimental phenomena, where the details of each reaction can be easily formulated, including the processes of well-known oxidation–addition and reduction–elimination.<sup>17</sup>

**Spectral Characterizations.** As shown in Figure 1, all new heterocyclic aromatic compounds show characteristic absorptions at 346–425 nm in their electronic spectra corresponding to the  $\pi$ – $\pi^*$  transitions between adjacent aromatic heterocycles in the asymmetrical D– $\pi$ –A and symmetrical D– $\pi$ –D system. It is noted that the conjugated thiazole molecules have a high molar absorption coefficient ( $>10\,000\text{ L}\cdot\text{mol}^{-1}\cdot\text{cm}^{-1}$ ) because of their unique D–A structures. Furthermore, this family of linear asymmetrical/symmetrical heterocyclic aromatic compounds is fluorescent-active from blue to yellow to green (446–566 nm). In particular, compound 2 shows an extraordinarily strong fluorescence peak at 488 nm with the luminescence quantum yield ( $\Phi$ ) of 41% (Table 1) (see the Supporting Information for details). At the same time, it exhibits a strong UV–vis absorption peak at 398 nm ( $\epsilon = 35\,700\text{ L}\cdot\text{mol}^{-1}\cdot\text{cm}^{-1}$ ). In comparison with compound 1, similar bathochromic shifts have been found in the fluorescence emission spectra of compounds 2, 3, 5–8, and 10–12 when the delocalized  $\pi$ -system of molecules is increased. Compared with compound 5, it is noted that its structural isomer compound 10 shows bathochromic shifts of 6 and 32 nm in the electronic absorption and luminescence spectra, respectively, which are in good agreement with the following theoretical studies. The luminescence quantum yield studies indicate that compounds 3, 5, 9, and 10 show low values of  $\Phi_s$  ( $<10\%$ ) because of the fluorescence quenching effects of the bromo and/or pyridyl groups.<sup>18</sup>

**Single-Crystal and Molecular Packing Structures of 2, 3, 5, and 7–9.** To have deeper insight into the molecular geometry and interesting supramolecular interactions, we tried

to obtain as many as single-crystal structures of our compounds. As a result, six asymmetrical D– $\pi$ –A and symmetrical D– $\pi$ –D types of thiazole-containing triphenylamino compounds, that is, 2, 3, 5, and 7–9 (Table 2 and Table SII, Supporting Information), have been structurally characterized. All six compounds crystallize in the same triclinic  $P\bar{1}$  space group, indicative of the low symmetry of molecules. The molecular lengths of compounds 2, 3, 5, 7, and 8 are longer than 1.30 nm. The two sulfur atoms from the thiazole ring and its neighboring thiophene ring in 7 and 8 are found to point to the opposite directions, exhibiting the common *trans* configuration with very small dihedral angles of  $1.2(3)^\circ$  or  $3.0(3)^\circ$  in 7 and  $0^\circ$  in 8. The thiazole core exhibits distinguishable dihedral angles with its adjacent benzene ring of the triphenylamino group in the range of  $3.6(3)$ – $40.8(3)^\circ$ , as shown in Figure 2. The C–C bond length between the triphenylamino and thiazolyl units in six compounds is ca. 1.46 Å, exhibiting a somewhat double-bond character.

The crystal packing view of this family of linear heterocyclic aromatic compounds 2, 3, 5, and 7–9 is shown in Figure SII2 (Supporting Information). It is worth mentioning that the packing structure of 9 has the  $\pi$ – $\pi$  stacking interactions between neighboring thiazole and pyridine rings with the centroid-to-centroid separation of 3.846(1) Å. However, strong  $\pi$ – $\pi$  stacking interactions are not observed in the other five TPA-functionalized molecules mainly because of the steric hindrance effects of large triphenylamino groups.

**Thermal Stability.** In this work, eleven thiazole-based aromatic heterocyclic compounds have been checked by the TGA measurements and a parameter of  $T_{d_{10}}$  (10% weight-loss temperature) is used to describe the thermal durability of these compounds (Table 1). In general, the thermal stability of heterocyclic aromatic compounds has an important impact on the device performance based on the thermal annealing method, which is one of the most essential parameters for the fine-tuned optoelectronic applicability.<sup>19</sup> However,  $\pi$ -conjugated organic compounds with the  $T_{d_{10}}$  value higher than  $400^\circ\text{C}$  are not very common. Therefore, according to the lessons learned from those successful or unsuccessful examples,<sup>12f–h</sup> we have reconsidered the molecular design and try to come up with a solution to increase the thermal stability of our compounds. The introduction of triphenylamino chromophores with a strong donor property is found to be an efficient approach in this work.

The TGA curves of 1–3, 5–8, and 10–12 indicate that they can remain unchangeable when the temperature is below 250

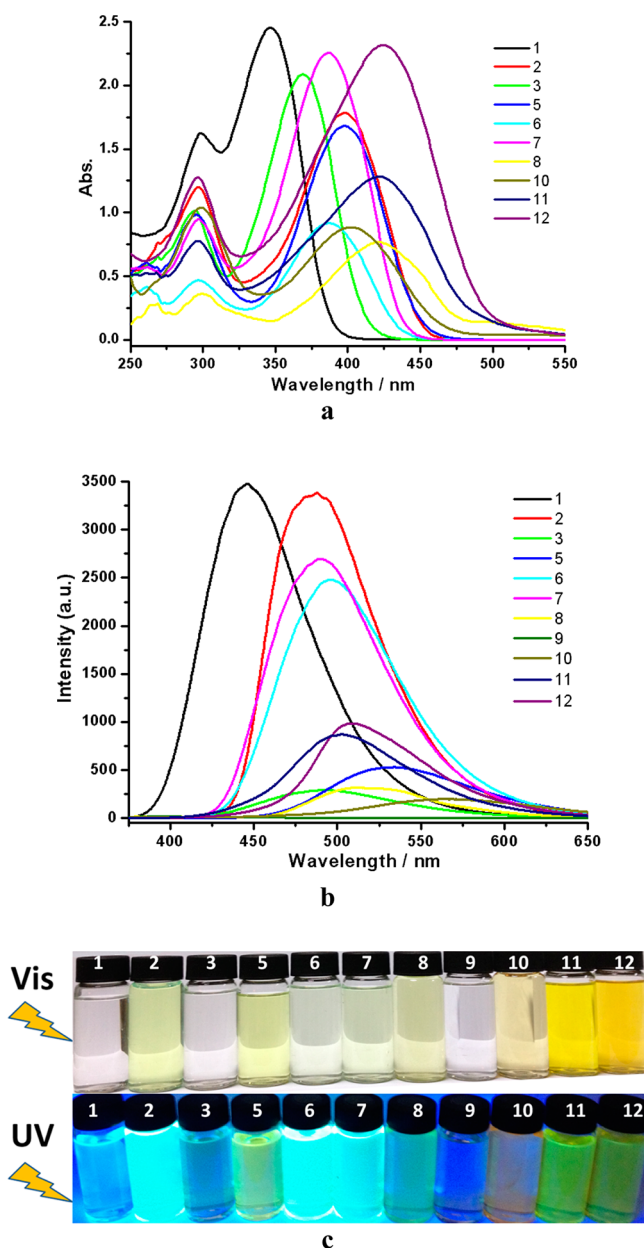


**Figure 1.** UV–vis absorption spectra (a), fluorescence emission excited at 350 nm (b), and their visual photographs (c) for the thiazole-containing triphenylamino compounds in their methanol solutions at room temperature with the same concentration of  $5.0 \times 10^{-5} \text{ mol}\cdot\text{L}^{-1}$ .

$^{\circ}\text{C}$  and the  $T_{d_{10}}$  values for them are found to range from 271 to  $503^{\circ}\text{C}$  in Figure 3. Moreover, the thiazole derivatives **2** and **5–8** show higher thermal stability compared with other thiazole-containing compounds. It is noted that the  $T_{d_{10}}$  value for the TPA-extended bithiazole compound **8** reaches as high as  $503^{\circ}\text{C}$ , indicative of the excellent thermal stability. Compared with our previously reported compounds,<sup>12g</sup> this family of molecules shows enhanced thermal stability due, in large part, to the removal of two *n*-butyl alkyl chains in the central bithiazole units and the increase of crystallization characteristics on the premise of keeping solubility in organic solvents.

**Electrochemical Properties.** To further reveal the electrochemical activity and energy level information, the electrochemical behavior of thiazole-based heterocyclic aromatic

compounds was examined by the cyclic voltammetry (CV) and the differential pulse voltammetry (DPV) measurements in their  $1.0 \times 10^{-3} \text{ mol}\cdot\text{L}^{-1} \text{ CH}_2\text{Cl}_2$  solutions containing  $0.10 \text{ mol}\cdot\text{L}^{-1} \text{ TBAClO}_4$  as the supporting electrolyte at different scan rates (20, 50, 80, and  $100 \text{ mV/s}$ ). All potentials reported herein were calibrated with the ferrocene/ferrocenium couple ( $\text{Fc}/\text{Fc}^+$ ) as an internal standard. The oxidation onset potentials ( $E_{\text{ox}}^{\text{onset}}$ ) as well as the HOMO/LUMO energy levels were determined by the DPV and electronic spectral data, which are summarized in Table 1. The onset oxidation was measured relative to the  $\text{Fc}/\text{Fc}^+$  couple where an energy level of  $-5.10 \text{ eV}$  versus vacuum was assumed.<sup>20</sup>

As depicted in Figures 4a and SI15d (Supporting Information), compound **7** shows a reversible and well-defined redox response in the CV measurements. Besides, the DPV method is used to further explore the electrochemical properties for related compounds. As can be seen in Figure 4c, two or three oxidation waves have been observed for all compounds, and the oxidation potentials and the measured currents are found to be dependent on their molecular structures. For example, compound **7** displays three oxidation waves in the range of 0.5–1.1 V, indicative of the existence of three stable cation-radical species, which are suggested to be the first oxidation states of triphenylamine (0.51 V), thiophene (0.79 V), and thiazole (1.05 V).<sup>21</sup>

The first oxidation potentials  $E_{\text{ox}}^1$  of these  $\pi$ -functionalized thiazole compounds were determined to be 0.51 V for **7**, 0.52 V for **1**, 0.53 V for **6**, and 0.54 V for **10**, respectively. It is generally believed that the HOMO of the D–A oligomer is determined by the HOMO of the donor unit, whereas the LUMO of the D–A oligomer is controlled by the LUMO of the acceptor unit. TPA is known to be an efficient chromophore with a strong donor property.<sup>22</sup> Therefore, these molecules show similar HOMO energy levels in this case, which can guide us to rationally design the donor materials and finely tune the LUMO energy levels by means of introducing different electron-withdrawing groups for these TPA-based dyes.

**Density Function Theory (DFT) Computations.** DFT calculations are carried out with the Gaussian 09, revision C.01 program, using the B3LYP method and 6-31G\* basis set.<sup>23</sup> The fixed atom coordinates of 12 thiazole-containing compounds, which are based upon the structural parameters determined by the X-ray single-crystal diffraction method and the full optimization, are used for the HOMO and LUMO gap calculations (Table 1).

The resultant HOMO–LUMO gaps for thiazole-incorporated heterocyclic aromatic compounds **5** and **10** are 3.23 and 3.19 eV, respectively, which are analogous to their UV–vis absorption peaks. In addition, the DFT and DPV results show that compounds **5** and **10** have similar HOMO, but different LUMO, energy levels. It is believed that the introduction of electron-donating groups raises the HOMO energy levels, whereas the introduction of electron-withdrawing groups lowers the LUMO energy levels, which will greatly decrease the HOMO–LUMO gaps of resultant compounds. That is to say, the introduction of a pyridyl group at the 2-position of the thiazole unit is more effective than the 5-position in increasing the strength of D–A charge transfer for identical molecular formulas.

As shown in Figure 5, according to the DPV measurements, further analyses of the frontier orbitals reveal that there is a nearly linear relationship between the experimentally determined energy levels (DPV and UV–vis absorption spectra) and

**Table 1.** UV–vis Absorption and Fluorescence Emission Data, Optical, Electrochemistry, Calculated HOMO–LUMO Energy Gaps ( $E_g$ ), and Internal Reorganization Energy ( $\lambda$ ) for Related Heterocyclic Aromatic Compounds

compd	UV–vis $\lambda_{\max}$ [nm (eV)]	$\epsilon$ (L·mol <sup>-1</sup> ·cm <sup>-1</sup> )	$E_g^{\text{opt}a}$ (eV)	$E_g^{\text{calcd}b}$ (eV)	fluorescence		$T_{d_{10}}^d$ (°C)	$E_{\text{ox}}^{\text{onset}e}$ (V)	$E_{\text{HOMO}}^f$ (eV)	$E_{\text{LUMO}}^g$ (eV)	$\lambda_{\text{TZ}}^h$ (eV)	$\lambda_{\text{T}}^i$ (eV)
					$\lambda_{\max}$ (nm)	$\Phi_s^c$						
1	346 (3.58)	49 100	3.21	3.83	446	0.53	315	0.40	-5.50	-2.29	0.17	0.23
2	398 (3.12)	35 700	2.77	3.57	488	0.41	399	0.26	-5.36	-2.59	0.27	0.35
3	369 (3.36)	41 800	3.01	3.27	493	0.04	271	0.47	-5.57	-2.56	0.12	0.22
5	397 (3.12)	33 600	2.76	3.23	534	0.07	354	0.38	-5.48	-2.72	0.13	0.21
6	387 (3.20)	18 400	2.84	3.11	496	0.40	442	0.36	-5.46	-2.62	0.16	0.23
7	387 (3.20)	45 100	2.85	3.26	490	0.32	349	0.39	-5.49	-2.64	0.21	0.29
8	422 (2.94)	15 500	2.53	2.93	510	0.20	503	0.33	-5.43	-2.90	0.23	0.34
9	306 (4.05)	4910	3.56	4.44	396	0.02	190	1.07	-6.17	-2.61	0.37	0.38
10	403 (3.08)	17 800	2.64	3.19	566	0.03	329	0.40	-5.50	-2.86	0.18	0.21
11	421 (2.94)	25 800	2.50	2.75	503	0.16	323	0.25	-5.35	-2.85	0.23	0.32
12	425 (2.92)	46 500	2.47	2.64	509	0.16	318	0.34	-5.44	-2.97	0.23	0.29

<sup>a</sup>Optical energy gaps determined from the UV–vis absorptions in their methanol solutions. <sup>b</sup>The geometries are calculated by the B3LYP method and 6-31G\* basis set. <sup>c</sup>Photoluminescence quantum yields. <sup>d</sup>10% weight-loss temperature. <sup>e</sup>Oxidation onset potentials determined from DPV. <sup>f</sup>Calculated from  $E_{\text{HOMO}} = -(E_{\text{ox}}^{\text{onset}} + 5.10)$ . <sup>g</sup>Calculated from  $E_{\text{LUMO}} = E_{\text{HOMO}} + E_g^{\text{opt}}$ . <sup>h</sup>Calculated internal reorganization energy for thiazole-containing compounds. <sup>i</sup>Calculated internal reorganization energy for thiophene-based compounds.

**Table 2.** Crystal Data and Structure Refinement Details for Six Compounds 2, 3, 5, and 7–9

compd	2·EtOH·CHCl <sub>3</sub>	3	(5) <sub>2</sub> ·CH <sub>3</sub> CN	7	8·2H <sub>2</sub> O	9
formula	C <sub>42</sub> H <sub>36</sub> N <sub>3</sub> SOCl <sub>3</sub>	C <sub>21</sub> H <sub>13</sub> BrN <sub>2</sub> S	C <sub>54</sub> H <sub>41</sub> N <sub>7</sub> S <sub>2</sub>	C <sub>25</sub> H <sub>18</sub> N <sub>2</sub> S <sub>2</sub>	C <sub>42</sub> H <sub>34</sub> N <sub>4</sub> S <sub>2</sub> O <sub>2</sub>	C <sub>8</sub> H <sub>5</sub> BrN <sub>2</sub> S
formula wt	737.16	407.32	852.06	410.55	690.85	241.11
T (K)	291(2)	291(2)	291(2)	291(2)	291(2)	291(2)
wavelength (Å)	0.71073	0.71073	0.71073	0.71073	0.71073	0.71073
cryst size (mm)	0.10 × 0.10 × 0.10	0.16 × 0.18 × 0.20	0.08 × 0.10 × 0.10	0.10 × 0.12 × 0.12	0.10 × 0.10 × 0.10	0.10 × 0.12 × 0.12
cryst syst	triclinic	triclinic	triclinic	triclinic	triclinic	triclinic
space group	P $\bar{1}$	P $\bar{1}$	P $\bar{1}$	P $\bar{1}$	P $\bar{1}$	P $\bar{1}$
a (Å)	10.020(7)	10.0378(9)	10.2017(14)	10.3933(10)	10.237(4)	5.8778(18)
b (Å)	10.250(7)	10.1977(9)	12.9072(17)	12.6851(12)	11.233(4)	7.415(2)
c (Å)	18.583(13)	10.4509(9)	17.458(2)	16.6669(16)	15.634(5)	9.975(3)
$\alpha$ (deg)	78.568(11)	71.289(2)	85.786(2)	97.372(2)	78.122(4)	84.049(5)
$\beta$ (deg)	87.828(11)	72.671(2)	85.243(2)	105.335(1)	85.747(5)	87.505(5)
$\gamma$ (deg)	75.839(12)	65.066(1)	73.689(2)	98.675(2)	79.296(5)	77.632(4)
V (Å <sup>3</sup> )	1814(2)	902.18(14)	2195.6(5)	2062.0(3)	1727.5(11)	422.3(2)
Z/D <sub>calcd</sub> (g/cm <sup>3</sup> )	2/1.350	2/1.499	2/1.289	4/1.322	2/1.328	2/1.896
F(000)	768	412	892	856	724	236
$\mu$ (mm <sup>-1</sup> )	0.349	2.399	0.168	0.272	0.198	5.052
max/min transmission	0.9660/0.9660	0.7001/0.6455	0.9867/0.9834	0.9733/0.9681	0.9805/0.9805	0.6320/0.5824
$h_{\min}/h_{\max}$	-11/11	-11/11	-7/12	-9/12	-7/12	-6/6
$k_{\min}/k_{\max}$	-12/10	-10/12	-15/15	-15/14	-13/13	-8/8
$l_{\min}/l_{\max}$	-22/22	-12/12	-20/20	-19/19	-18/18	-11/7
data/parameter	6296/479	3153/226	7596/569	7162/542	5977/445	1460/109
final R indices [ $I > 2\theta(I)$ ] <sup>a</sup>	R1 = 0.0894 wR2 = 0.2226	R1 = 0.0411 wR2 = 0.0982	R1 = 0.0654 wR2 = 0.1805	R1 = 0.0495 wR2 = 0.1338	R1 = 0.0719 wR2 = 0.1948	R1 = 0.0526 wR2 = 0.1373
R indices (all data) <sup>a</sup>	R1 = 0.1228 wR2 = 0.2537	R1 = 0.0529 wR2 = 0.1013	R1 = 0.0994 wR2 = 0.2037	R1 = 0.0887 wR2 = 0.1520	R1 = 0.0849 wR2 = 0.2038	R1 = 0.0574 wR2 = 0.1404
S	0.95	0.93	0.97	1.03	1.02	1.01
max./min. $\Delta\rho$ [e·Å <sup>-3</sup> ]	1.36/-0.51	0.32/-0.49	0.29/-0.59	0.18/-0.25	1.63/-1.25	0.76/-1.15

<sup>a</sup>R1 =  $\sum ||F_o| - |F_c|| / \sum |F_o|$ , wR2 =  $[\sum [w(F_o^2 - F_c^2)^2] / \sum w(F_o^2)]^{1/2}$ .

the theoretically calculated ones for the HOMOs and LUMOs of these thiazole-containing heterocyclic aromatic hybrids, which is consistent with our previous work.<sup>12g</sup> On the one hand, these molecules show similar HOMO energy levels because of the presence of a strong electron-donating group of the TPA chromophore. On the other hand, increasing the conjugated molecular length and enhancing the strength of electron-withdrawing groups greatly lower the LUMO energy levels and partly decrease the HOMO–LUMO gaps of

resultant compounds simultaneously. More importantly, this relationship demonstrates that, despite the uncertainty in the calculated absolute values, theoretical calculations can act as a very useful tool to predict and guide the synthesis of future thiazole-based oligomer materials.

To make further comparisons from a theoretical and experimental perspective, investigations of the internal reorganization energy ( $\lambda$ ) have been done at the B3LYP/6-31G\* level for a series of  $\pi$ -conjugated thiazole-based

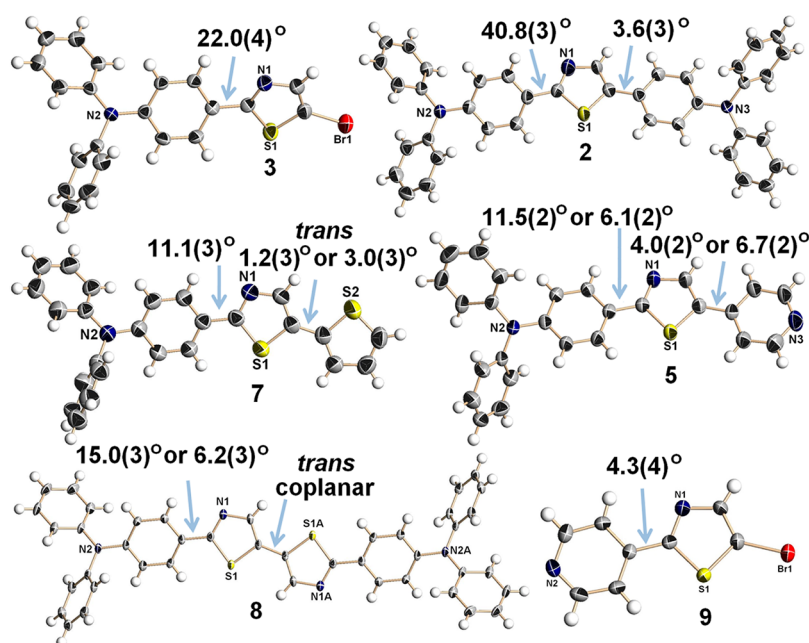


**Figure 2.** ORTEP diagrams (30% thermal probability ellipsoids) of the molecular structures of 2, 3, 5, and 7–9 showing the dihedral angles and relative configurations between adjacent aromatic heterocycles. The solvent molecules are omitted for clarity.

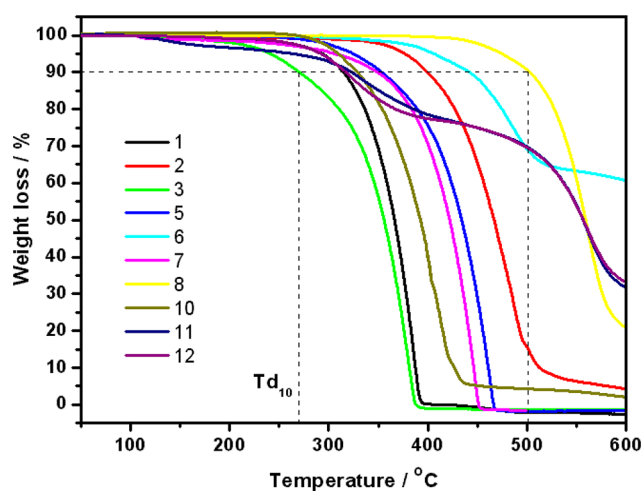


**Figure 3.** Thermograms of thiazole-containing triphenylamino compounds 1–3, 5–8, and 10–12.

derivatives and the corresponding thiophene-based counterparts. According to Marcus theory,<sup>24</sup> the self-exchange rate and the charge mobility are determined by the electronic coupling between adjacent molecules ( $t$ ), which needs to be maximized, and the reorganization energy ( $\lambda$ ), which needs to be small for efficient charge transport.<sup>9f</sup> The reorganization energy ( $\lambda$ ) depicts the changes in the geometry of two molecules during the electron-transfer reaction. It has two contributions, that is, an internal one and an external one. The contribution of the environmental factor (intermolecular) to the reorganization energy is expected to be small in an organic solid, and hence, only the intramolecular reorganization energy is calculated.<sup>25</sup> In this paper, the thiazole derivatives exhibit a slightly smaller internal reorganization energy than the thiophene counterparts, which means that the former may be good candidates for investigations of the design and synthesis of  $\pi$ -conjugated oligomers for OFET materials from a theoretical and experimental perspective. Comparatively speaking, the thia-

zole-containing triphenylamino chromophore compounds have smaller  $\lambda$  values, which can be explained commendably by the presence of intermolecular hydrogen bonds and/or small dihedral angles between the thiazole and the thiophene/benzene/pyridine rings in their crystal structures.

**Solid-State Conductance Properties.** To further reveal the solid-state conductance of linear aromatic heterocyclic compounds 11 and 12, two ends of their solid samples are covered by a pair of electrodes made of conductive silver paste, and the corresponding  $I$ – $V$  curves are recorded between the pair of electrodes by means of a four-probe system under the same experimental condition for comparison. As shown in Figure 6, linear fitting of the two obtained  $I$ – $V$  curves gave the average resistivity of  $1.3 \times 10^6 \Omega\cdot\text{m}$  for compound 11 and  $1.1 \times 10^6 \Omega\cdot\text{m}$  for compound 12, exhibiting typical semiconducting characteristics. The better conjugacy for the central thiophene/thiazole extended aromatic rings as well as the abundant supramolecular interactions, such as S...S contact, hydrogen bonding, and  $\pi$ – $\pi$  stacking, plays important roles in increasing the conductivity of compounds 11 and 12, because the solid-state conductance of semiconducting compounds strongly relies on the delocalized  $\pi$ -system of the whole molecules and their packing fashions. Compared with compound 11, the enhancement of solid-state conductance for compound 12 is mainly ascribed to its lower band gap (2.75 and 2.64 eV for compounds 11 and 12, as depicted in Table 1).

## CONCLUSION

In summary, a family of thermally stable and soluble thiazole-based heterocyclic aromatic fluorescent compounds having the same triphenylamino chromophores are described herein. All of these multiple N-donor-containing compounds have effective  $\pi$ -conjugated systems and different triphenylamino, pyridine, thiophene, and benzoic acid tails showing symmetrical D– $\pi$ –D and asymmetrical D– $\pi$ –A structures. Investigations of the differences between the coupling approaches and experimental conditions on C–C bond formation and C–H bond activation;

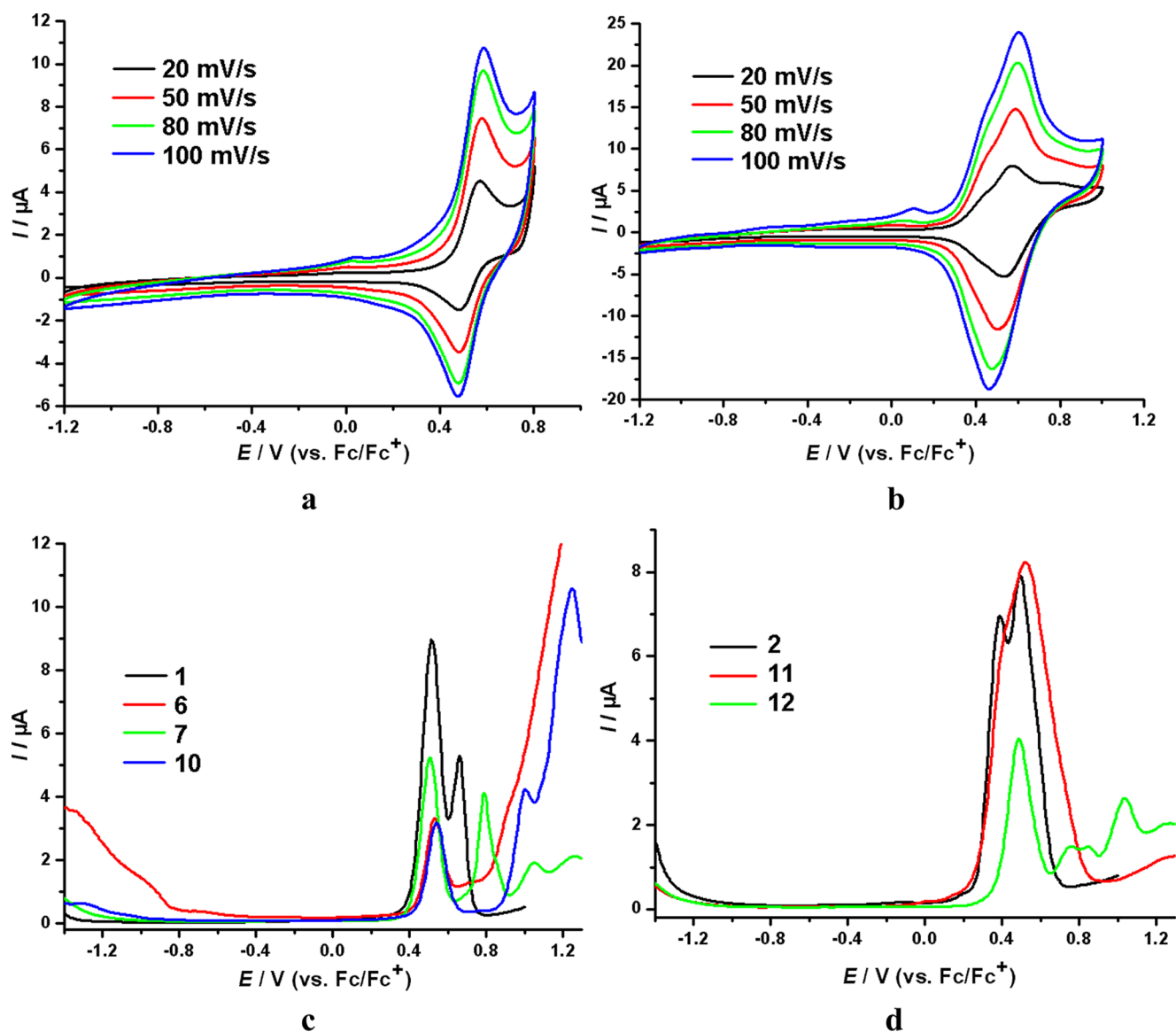


**Figure 4.** CV (a, b) and DPV (c, d) for related heterocyclic aromatic compounds in  $\text{CH}_2\text{Cl}_2$  ( $1.0 \times 10^{-3} \text{ mol}\cdot\text{L}^{-1}$ ) containing  $0.10 \text{ mol}\cdot\text{L}^{-1}$  of  $\text{TBAClO}_4$  under argon. In CV, different scanning rates of 20, 50, 80, and  $100 \text{ mV}\cdot\text{s}^{-1}$  are used for compounds 7 (a) and 11 (b) vs  $\text{Fc}/\text{Fc}^+$ .

the molecular conformation and dihedral angles between neighboring heterocycles; the energy gaps and energy levels; the thermal stability; the electronic, fluorescence, and electrochemistry spectra; and the DFT computations have been systematically carried out.

It is interesting to mention that compound 2 can be prepared by the Suzuki–Miyaura coupling and subsequent C–H activation from a 5-TPA-substituted thiazole intermediate 1 via a one-pot reaction, where a possible two-step reaction mechanism is given based on the distinguishable reaction activity for 2- and 5-positions of one thiazole ring. X-ray single-crystal structures of six compounds indicate that they all crystallize in the same triclinic  $P\bar{1}$  space group and the thiazole cores exhibit different dihedral angles with their adjacent benzene ring of the triphenylamino group ( $3.6(3)$ – $40.8(3)^\circ$ ). Fluorescence spectral studies reveal that compounds 1, 2, and 6 show high luminescence quantum yields ( $\Phi_s = 40$ – $53\%$ ). Moreover, the electrochemical results demonstrate that compound 7 exhibits high electrochemical activity, and the

TGA studies indicate that compound 8 has excellent thermal stability with a  $T_{d_{10}}$  value as high as  $503^\circ\text{C}$ .

The acquirement of these linear symmetrical/asymmetrical heterocyclic aromatic compounds, especially the single-crystal structures, promotes us to further explore the possible rules between their structures and properties. Therefore, the theoretical and experimental studies have been made to reveal the differences from related compounds with adjustable electronic properties. Comparatively speaking, the thiazole derivatives exhibit a slightly smaller internal reorganization energy than the corresponding thiophene units, which suggests that the former may be good candidates for investigations of the design and synthesis of new  $\pi$ -conjugated oligomers for OFET materials from a theoretical and experimental perspective. Further studies are being undertaken on the field-effect, light-emitting, photoresponsive, and photovoltaic properties of these linear multiple N-donor-containing aromatic heterocycle-based nanowires, nanocomposite films, and nano-devices in our laboratory.

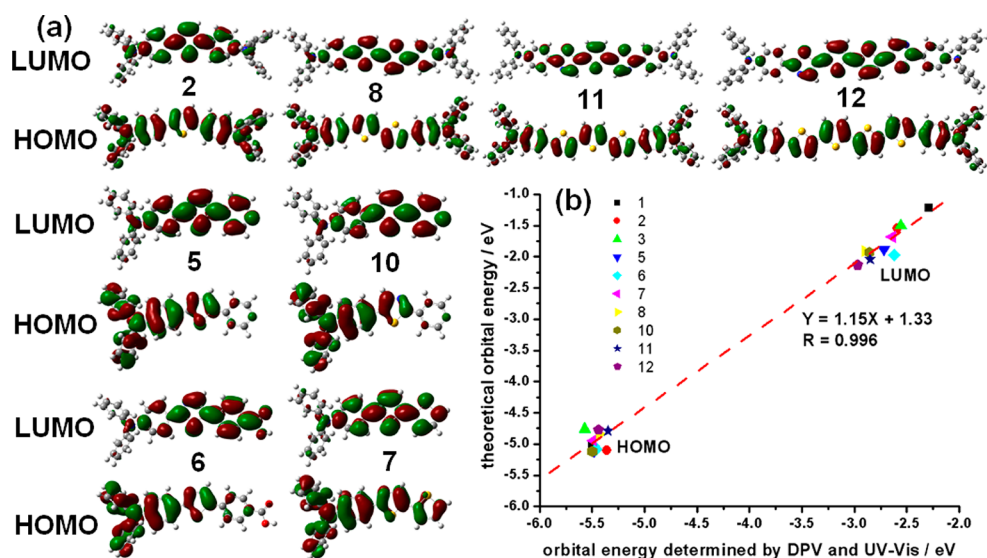


Figure 5. (a) HOMOs and LUMOs of 2, 5–8, and 10–12 calculated with B3LYP/6-31G\*. (b) Energy level correlation between the DPV, UV–vis absorption spectra, and the computational data.

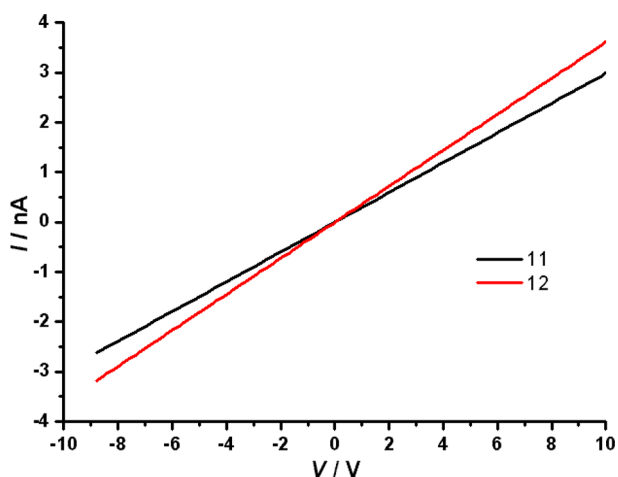


Figure 6. *I*–*V* curves for two narrow band gap semiconducting compounds 11 and 12 in the solid state at room temperature.

## EXPERIMENTAL SECTION

**Syntheses and Characterizations of Heterocyclic Aromatic Compounds 1–3 and 5–12.** *Compounds 1 and 2.* A mixture of 5-bromothiazole (0.16 g, 1.00 mmol), 4-(diphenylamino)phenylboronic acid (0.58 g, 2.00 mmol), [Pd(PPh<sub>3</sub>)<sub>4</sub>] (0.06 g, 0.05 mmol), cesium carbonate (0.65 g, 2.00 mmol), toluene (20 mL), and water (4 mL) was degassed for 10 min and heated to reflux for 48 h under an argon atmosphere. The mixture was then allowed to cool to the room temperature and extracted with chloroform. The resulting organic layer was dried with anhydrous sodium sulfate and filtered. Compounds 1 and 2 were purified by silica gel column chromatography using hexane and dichloromethane (2:1) as an eluent to give the yellow solid in yields of 0.20 g (61%) for 1 and 0.07 g (12%) for 2, respectively. 1: mp 133–134 °C. Main FT-IR absorptions (KBr pellets, cm<sup>-1</sup>): 3442 (b), 1589 (s), 1527 (m), 1487 (s), 1322 (m), 1275 (s), 1110 (w), 874 (w), 835 (m), 757 (s), 694 (s), 513 (m). <sup>1</sup>H NMR (500 MHz, CDCl<sub>3</sub>): δ 8.69 (s, 1H, thiazolyl), 7.99 (s, 1H, thiazolyl), 7.42 (d, 2H, *J* = 8.4 Hz, triphenylamino), 7.28–7.26 (t, 4H, triphenylamino), 7.12 (d, 4H, *J* = 8.2 Hz, triphenylamino), 7.08–7.04 (m, 4H, triphenylamino). <sup>13</sup>C NMR (125 MHz, CDCl<sub>3</sub>): δ 151.3, 148.2, 147.3, 139.4, 138.1, 129.4, 127.8, 124.8, 124.6, 123.5, 123.3. EI-TOF-MS (*m/z*): calcd for [C<sub>21</sub>H<sub>16</sub>N<sub>2</sub>S]<sup>+</sup> 328.1 (100.0), 329.1 (22.9), found 328.0 (100.0), 329.0 (11.6). Anal. calcd for C<sub>21</sub>H<sub>16</sub>N<sub>2</sub>S: C,

76.80; H, 4.91; N, 8.53%. Found: C, 76.68; H, 5.03; N, 8.41%. The yellow single crystals of compound 2 suitable for X-ray diffraction determination were grown from a mixed solution of chloroform and ethanol (v/v = 1:1) by slow evaporation in air at room temperature for 1 week. 2: mp > 250 °C. Main FT-IR absorptions (KBr pellets, cm<sup>-1</sup>): 3437 (b), 1585 (s), 1480 (s), 1410 (m), 1325 (m), 1273 (m), 1183 (m), 1112 (w), 965 (w), 869 (m), 753 (m), 697 (s), 623 (w). <sup>1</sup>H NMR (500 MHz, CDCl<sub>3</sub>): δ 7.88 (s, 1H, thiazolyl), 7.80 (d, 2H, *J* = 8.8 Hz, triphenylamino), 7.44 (d, 2H, *J* = 8.6 Hz, triphenylamino), 7.31–7.27 (m, 8H, triphenylamino), 7.15–7.12 (t, 8H, triphenylamino), 7.09–7.04 (m, 8H, triphenylamino). <sup>13</sup>C NMR (125 MHz, CDCl<sub>3</sub>): δ 166.2, 149.5, 147.9, 147.3, 147.1, 138.2, 138.1, 129.4, 127.4, 127.2, 125.1, 124.7, 123.7, 123.4, 122.4. EI-TOF-MS (*m/z*): calcd for [C<sub>39</sub>H<sub>29</sub>N<sub>3</sub>S]<sup>+</sup> 571.2 (100.0), 572.2 (44.4), found 571.1 (100.0), 572.1 (51.0). Anal. calcd for C<sub>39</sub>H<sub>29</sub>N<sub>3</sub>S: C, 81.93; H, 5.11; N, 7.35%. Found: C, 81.67; H, 5.19; N, 7.21%.

*Compounds 2 and 3.* These compounds were synthesized according to the above procedure by minor modifications. The contents of a degassed three-neck flask containing 2,5-dibromothiazole (0.97 g, 4.00 mmol), 4-(diphenylamino)phenylboronic acid (1.73 g, 6.00 mmol), [Pd(PPh<sub>3</sub>)<sub>4</sub>] (0.12 g, 0.10 mmol), and cesium carbonate (1.95 g, 6.00 mmol) were dissolved in a degassed mixture of toluene (50 mL) and water (5 mL). The mixture was stirred and heated to reflux for 48 h under an argon atmosphere. The mixture was then allowed to cool to the room temperature and extracted with chloroform. The resulting organic layer was dried over anhydrous sodium sulfate and filtered. Compounds 2 and 3 were purified by silica gel column chromatography using hexane and dichloromethane (v/v = 1:1) as an eluent to give the yellow solid in yields of 0.41 g (18%) for 2 and 1.09 g (67%) for 3, respectively. 2: see the above. The yellow single crystals of compound 3 suitable for X-ray diffraction determination were grown from a solution of chloroform by slow evaporation in air at room temperature for 4 days. 3: mp > 250 °C. Main FT-IR absorptions (KBr pellets, cm<sup>-1</sup>): 3437 (b), 1583 (s), 1481 (s), 1331 (m), 1269 (m), 758 (m), 695 (s). <sup>1</sup>H NMR (500 MHz, CDCl<sub>3</sub>): δ 7.70 (s, 1H, thiazolyl), 7.67 (d, 2H, *J* = 7.4 Hz, triphenylamino), 7.31–7.28 (t, 4H, triphenylamino), 7.14 (d, 4H, *J* = 7.6 Hz, triphenylamino), 7.11–7.08 (t, 2H, triphenylamino), 7.05 (d, 2H, *J* = 8.8 Hz, triphenylamino). <sup>13</sup>C NMR (125 MHz, CDCl<sub>3</sub>): δ 169.5, 150.0, 147.0, 144.6, 129.5, 127.2, 126.3, 125.3, 124.0, 122.0, 107.2. EI-TOF-MS (*m/z*): calcd for [C<sub>21</sub>H<sub>15</sub>BrN<sub>2</sub>S]<sup>+</sup> 408.0 (100.0), 406.0 (98.1), found 408.0 (75.3), 406.0 (100.0). Anal. calcd for C<sub>21</sub>H<sub>15</sub>BrN<sub>2</sub>S: C, 61.92; H, 3.71; N, 6.88%. Found: C, 61.68; H, 3.83; N, 6.72%.



**Compound 5.** A mixture of compound **3** (0.41 g, 1.00 mmol), 4-pyridinylboronic acid (0.15 g, 1.20 mmol), cesium carbonate (0.39 g, 1.20 mmol), [Pd(PPh<sub>3</sub>)<sub>4</sub>] (0.06 g, 0.05 mmol), dioxane (30 mL), and water (5 mL) was degassed for 0.5 h and heated to reflux for 40 h under an argon atmosphere. After the mixture was cooled to room temperature, chloroform (50 mL) was added, and the organic phase was washed with brine, separated, and dried over anhydrous sodium sulfate. The organic solvent was evaporated under reduced pressure, and the solid residue was purified by silica gel column chromatography using a mixture of hexane and dichloromethane (v/v = 1:2) as an eluent to provide the desired product **5** as a dark yellow solid in a yield of 0.36 g (89%). The yellow single crystals of compound **5** suitable for X-ray diffraction determination were grown from a mixed solution of chloroform and acetonitrile (v/v = 1:1) by slow evaporation in air at room temperature for 3 weeks. **5**: mp 208–210 °C. Main FT-IR absorptions (KBr pellets, cm<sup>-1</sup>): 3442 (b), 1589 (s), 1486 (s), 1433 (m), 1415 (s), 1331 (m), 1291 (s), 1265 (m), 1184 (m), 817 (m), 755 (m), 702 (s), 614 (m), 543 (m). <sup>1</sup>H NMR (500 MHz, CDCl<sub>3</sub>): δ 8.63 (d, 2H, J = 4.4 Hz, pyridyl), 8.16 (s, 1H, thiazolyl), 7.81 (d, 2H, J = 8.5 Hz, triphenylamino), 7.48 (d, 2H, J = 5.0 Hz, pyridyl), 7.33–7.29 (t, 4H, triphenylamino), 7.16 (d, 4H, J = 8.0 Hz, triphenylamino), 7.13–7.10 (t, 2H, triphenylamino), 7.08 (d, 2H, J = 8.6 Hz, triphenylamino). <sup>13</sup>C NMR (125 MHz, CDCl<sub>3</sub>): δ 169.6, 150.3, 149.8, 146.8, 141.7, 139.7, 134.6, 129.6, 127.9, 126.1, 125.4, 124.1, 121.7, 120.6. EI-TOF-MS (*m/z*): calcd for [C<sub>26</sub>H<sub>19</sub>N<sub>3</sub>S]<sup>+</sup> 405.1 (100.0), 406.1 (30.6), found 405.1 (100.0), 406.1 (19.6). Anal. calcd for C<sub>26</sub>H<sub>19</sub>N<sub>3</sub>S: C, 77.01; H, 4.72; N, 10.36%. Found: C, 76.79; H, 4.86; N, 10.20%.

**Compound 6.** The contents of a degassed three-neck flask containing compound **3** (1.63 g, 4.00 mmol), 4-boronobenzoic acid (0.73 g, 4.40 mmol), cesium carbonate (1.95 g, 6.00 mmol), and [Pd(PPh<sub>3</sub>)<sub>4</sub>] (0.12 g, 0.10 mmol) were dissolved in a degassed dioxane/water mixture (55 mL, 10:1). The mixture was stirred and refluxed under argon for 28 h. After being cooled to room temperature, the light yellow solid was obtained in the reaction mixture. The precipitate was filtered, washed with CHCl<sub>3</sub> and methanol, and then dried in vacuo to produce compound **6** in a yield of 1.52 g (85%). mp 241–245 °C. Main FT-IR absorptions (KBr pellets, cm<sup>-1</sup>): 3429 (b), 1591 (s), 1544 (m), 1481 (m), 1395 (s), 1329 (m), 1277 (m), 699 (m). <sup>1</sup>H NMR (500 MHz, CD<sub>3</sub>OD): δ 8.18 (s, 1H, thiazolyl), 8.08 (d, 2H, J = 8.2 Hz, phenyl), 7.83 (d, 2H, J = 8.5 Hz, triphenylamino), 7.77 (d, 2H, J = 7.4 Hz, phenyl), 7.36–7.33 (t, 4H, triphenylamino), 7.14 (d, 4H + 2H, J = 7.8 Hz, triphenylamino), 7.14 (d, 2H, J = 8.4 Hz, triphenylamino). <sup>13</sup>C NMR (125 MHz, CD<sub>3</sub>OD): δ 169.3, 151.4, 148.2, 140.3, 131.2, 130.6, 130.5, 130.2, 128.8, 128.3, 126.7, 126.4, 125.2, 122.5. EI-TOF-MS (*m/z*): calcd for [C<sub>28</sub>H<sub>20</sub>N<sub>2</sub>O<sub>2</sub>S]<sup>+</sup> 448.5, found 448.1. Anal. calcd for C<sub>28</sub>H<sub>20</sub>N<sub>2</sub>O<sub>2</sub>S: C, 74.98; H, 4.49; N, 6.25%. Found: C, 74.75; H, 4.53; N, 6.13%.

**Compound 7.** A mixture of compound **3** (0.81 g, 2.00 mmol), 2-thiophenylboronic acid (0.28 g, 2.20 mmol), cesium carbonate (0.72 g, 2.20 mmol), [Pd(PPh<sub>3</sub>)<sub>4</sub>] (0.12 g, 0.10 mmol), dioxane (50 mL), and water (5 mL) was degassed for 0.5 h and heated to reflux for 18 h under an argon atmosphere. After the mixture was cooled to room temperature, chloroform (50 mL) was added, and the organic phase was washed with brine, separated, and dried over anhydrous sodium sulfate. The organic solvent was evaporated under reduced pressure and the solid residue was purified by silica gel column chromatography using dichloromethane as an eluent to provide the desired product **7** as a dark yellow solid in a yield of 0.69 g (84%). The yellow single crystals of compound **7** suitable for X-ray diffraction determination were grown from a solution of chloroform by slow evaporation in air at room temperature for 5 days. mp 192–194 °C. Main FT-IR absorptions (KBr pellets, cm<sup>-1</sup>): 3435 (b), 1589 (s), 1487 (s), 1322 (m), 1275 (s), 1141 (w), 969 (w), 843 (m), 748 (m), 702 (s), 631 (w), 513 (w). <sup>1</sup>H NMR (500 MHz, CDCl<sub>3</sub>): δ 7.86 (s, 1H, thiazolyl), 7.80 (d, 2H, J = 8.6 Hz, triphenylamino), 7.31 (t, 4H, triphenylamino), 7.29 (d, 1H, J = 7.8 Hz, thienyl), 7.21 (d, 1H, J = 3.4 Hz, thienyl), 7.15 (d, 4H, J = 7.6 Hz, triphenylamino), 7.12–7.09 (t, 2H, triphenylamino), 7.07 (d, 2H, J = 8.8 Hz, triphenylamino), 7.05 (t, 1H, thienyl). <sup>13</sup>C NMR (125 MHz, CDCl<sub>3</sub>): δ 166.6, 149.8, 147.0, 139.0, 133.4, 131.3, 129.5, 127.9, 127.4, 125.4, 125.3, 123.9, 122.1. EI-

TOF-MS (*m/z*): calcd for [C<sub>25</sub>H<sub>18</sub>N<sub>2</sub>S<sub>2</sub>]<sup>+</sup> 410.1 (100.0), 411.1 (29.4), found 410.1 (100.0), 411.1 (12.2). Anal. calcd for C<sub>25</sub>H<sub>18</sub>N<sub>2</sub>S<sub>2</sub>: C, 73.14; H, 4.42; N, 6.82%. Found: C, 72.98; H, 4.58; N, 6.69%.

**Compound 8.** Compound **3** (0.45 g, 1.10 mmol), bis(pinacolato)-diboron (0.14 g, 0.55 mmol), and KOH (0.62 g, 11.00 mmol) were dissolved in a degassed dioxane/water mixture (24 mL, 5:1), argon was bubbled through the solution for 5 min, then the [Pd(PPh<sub>3</sub>)<sub>4</sub>] (0.06 g, 0.05 mmol) was added, and the reaction mixture was kept under stirring and refluxing for 10 h. After the mixture was cooled to room temperature, CHCl<sub>3</sub> (50 mL) was added, and the organic phase was washed with brine, separated, and dried over anhydrous Na<sub>2</sub>SO<sub>4</sub>. The organic solvent was evaporated under reduced pressure and the solid residue was purified by silica gel column chromatography using CHCl<sub>3</sub> as an eluent to provide the desired product **8** as a yellow solid in a yield of 0.28 g (78%). The red single crystals suitable for X-ray diffraction determination were grown from a solution of ethanol by slow evaporation in air at room temperature for 1 week. mp > 250 °C. Main FT-IR absorptions (KBr pellets, cm<sup>-1</sup>): 3437 (b), 1583 (s), 1481 (s), 1410 (m), 1323 (m), 1285 (s), 1143 (w), 758 (m), 696 (s). <sup>1</sup>H NMR (500 MHz, CDCl<sub>3</sub>): δ 7.85 (s, 2H, thiazolyl), 7.78 (d, 4H, J = 8.6 Hz, triphenylamino), 7.32–7.29 (t, 8H, triphenylamino), 7.15 (d, 8H, J = 8.2 Hz, triphenylamino), 7.12–7.09 (t, 4H, triphenylamino), 7.07 (d, 4H, J = 8.8 Hz, triphenylamino). <sup>13</sup>C NMR (125 MHz, CDCl<sub>3</sub>): δ 167.3, 149.9, 147.0, 140.7, 129.5, 127.5, 126.4, 125.3, 124.0, 122.0. EI-TOF-MS (*m/z*): calcd for [C<sub>42</sub>H<sub>30</sub>N<sub>4</sub>S<sub>2</sub>]<sup>+</sup> 654.2 (100.0), 655.2 (48.5), 656.2 (10.5), found 654.1 (100.0), 655.2 (66.0), 656.2 (4.0). Anal. calcd for C<sub>42</sub>H<sub>30</sub>N<sub>4</sub>S<sub>2</sub>: C, 77.03; H, 4.62; N, 8.56%. Found: C, 76.79; H, 4.76; N, 8.38%.

**Compound 9.** The contents of a degassed three-neck flask containing 2,5-dibromothiazole (2.43 g, 10.00 mmol), 4-pyridineboronic acid (1.35 g, 11.00 mmol), [Pd(PPh<sub>3</sub>)<sub>4</sub>] (0.24 g, 0.20 mmol), and Cs<sub>2</sub>CO<sub>3</sub> (3.91 g, 12.00 mmol) were dissolved in a degassed mixture of dioxane (50 mL) and H<sub>2</sub>O (5 mL). The mixture was stirred and refluxed under an argon atmosphere for 48 h. After the mixture was cooled to room temperature, CHCl<sub>3</sub> (100 mL) was added, and the organic phase was washed with brine, separated, and dried over anhydrous Na<sub>2</sub>SO<sub>4</sub>. The organic solvent was evaporated under reduced pressure and the solid residue was purified by silica gel column chromatography using CHCl<sub>3</sub> as an eluent to provide the desired product **9** as a light yellow solid in a yield of 1.81 g (75%). The yellow single crystals of **9** suitable for X-ray diffraction determination were grown from a solution of CHCl<sub>3</sub> by slow evaporation in air at room temperature for 4 days. mp 174–175 °C. Main FT-IR absorptions (KBr pellets, cm<sup>-1</sup>): 3421 (b), 1599 (s), 1544 (m), 1410 (s), 1308 (m), 1230 (m), 1112 (m), 994 (w), 868 (s), 814 (s), 703 (m), 562 (m). <sup>1</sup>H NMR (500 MHz, CDCl<sub>3</sub>): δ 8.73 (d, 2H, J = 5.1 Hz, pyridyl), 7.85 (s, 1H, thiazolyl), 7.76 (d, 2H, J = 5.6 Hz, pyridyl). <sup>13</sup>C NMR (125 MHz, CDCl<sub>3</sub>): δ 150.7, 145.7, 133.0, 132.1, 131.9, 128.5, 120.0. EI-TOF-MS (*m/z*): calcd for [C<sub>8</sub>H<sub>5</sub>BrN<sub>2</sub>S]<sup>+</sup> 241.9 (100.0), 239.9 (98.2), found 241.9 (88.2), 239.9 (100.0). Anal. calcd for C<sub>8</sub>H<sub>5</sub>BrN<sub>2</sub>S: C, 39.85; H, 2.09; N, 11.62%. Found: C, 39.67; H, 2.11; N, 11.54%.

**Compound 10.** Compound **9** (0.24 g, 1.00 mmol), 4-(diphenylamino)phenylboronic acid (0.29 g, 1.00 mmol), and cesium carbonate (0.32 g, 1.00 mmol) were dissolved in a degassed toluene/water mixture (24 mL, 5:1), argon was bubbled through the solution for 10 min, then the [Pd(PPh<sub>3</sub>)<sub>4</sub>] catalyst (0.06 g, 0.05 mmol) was added, and the reaction mixture was kept under stirring and refluxing for 36 h. The mixture was then allowed to cool to the room temperature and extracted with chloroform. The resulting organic layer was dried over anhydrous Na<sub>2</sub>SO<sub>4</sub> and filtered. The organic solvent was evaporated under reduced pressure and the solid residue was purified by silica gel column chromatography using CHCl<sub>3</sub> as an eluent to provide the desired product **10** as a green solid in a yield of 0.37 g (91%). mp > 250 °C. Main FT-IR absorptions (KBr pellets, cm<sup>-1</sup>): 3438 (b), 1583 (s), 1488 (s), 1436 (s), 1414 (s), 1289 (s), 1179 (s), 818 (m), 700 (s), 612 (m), 538 (s). <sup>1</sup>H NMR (500 MHz, CDCl<sub>3</sub>): δ 8.70 (d, 2H, J = 5.0 Hz, pyridyl), 8.01 (s, 1H, thiazolyl), 7.80 (d, 2H, J = 5.8 Hz, pyridyl), 7.53 (d, 2H, J = 7.5 Hz, triphenylamino), 7.30–7.27 (t, 4H, triphenylamino), 7.14 (d, 4H, J = 7.6 Hz, triphenylamino), 7.09 (m,

4H, triphenylamino).  $^{13}\text{C}$  NMR (125 MHz,  $\text{CDCl}_3$ ):  $\delta$  175.8, 159.5, 149.2, 146.9, 144.3, 139.9, 132.2, 129.5, 127.9, 125.2, 124.0, 123.0, 122.4, 121.4. EI-TOF-MS ( $m/z$ ): calcd for  $[\text{C}_{26}\text{H}_{19}\text{N}_3\text{S}]^+$  405.1 (100.0), 406.1 (30.0), found 405.1 (100.0), 406.1 (19.5). Anal. calcd for  $\text{C}_{26}\text{H}_{19}\text{N}_3\text{S}$ : C, 77.01; H, 4.72; N, 10.36%. Found: C, 76.81; H, 4.80; N, 10.24%.

**Compound 11.** A mixture of compound 3 (0.41 g, 1.00 mmol), 2,5-bis(trimethylstannyl)thiophene (0.20 g, 0.49 mmol), and the catalyst  $[\text{Pd}(\text{PPh}_3)_2\text{Cl}_2]$  (0.014 g, 0.02 mmol) was refluxed for 6 h in dry THF (20 mL) under an argon atmosphere. After the mixture was cooled to room temperature and evaporated under reduced pressure, the residue was dissolved in  $\text{CHCl}_3$ . The organic phase was washed twice with a saturated solution of  $\text{NaHCO}_3$  and then with water. After drying on  $\text{MgSO}_4$  and evaporation of solvent, the crude was purified by silica gel column chromatography using  $\text{CHCl}_3$  as an eluent to give compound 11 as the red solid (0.19 g, 54% yield). 11: mp > 250 °C. Main FT-IR absorptions (KBr pellets,  $\text{cm}^{-1}$ ): 3427 (b), 2971 (m), 1589 (m), 1487 (m), 1409 (m), 1047 (s), 882 (w), 748 (w), 694 (m).  $^1\text{H}$  NMR (500 MHz,  $\text{CDCl}_3$ ):  $\delta$  7.85 (s, 2H, thiazolyl), 7.78 (d, 4H,  $J = 8.4$  Hz, triphenylamino), 7.32–7.29 (t, 8H, triphenylamino), 7.15 (d, 8H,  $J = 8.0$  Hz, triphenylamino), 7.12 (s, 2H, thienyl), 7.10–7.07 (t, 8H, triphenylamino).  $^{13}\text{C}$  NMR (125 MHz,  $\text{CDCl}_3$ ):  $\delta$  166.8, 149.9, 149.8, 147.0, 140.7, 139.4, 129.5, 127.5, 127.4, 125.9, 125.3, 124.0, 122.0. EI-TOF-MS ( $m/z$ ): calcd for  $[\text{C}_{46}\text{H}_{32}\text{N}_4\text{S}_3]^+$  736.2 (100.0), 737.2 (53.6), 738.2 (13.6), found 736.2 (100.0), 737.2 (30.7), 738.2 (3.86). Anal. calcd for  $\text{C}_{46}\text{H}_{32}\text{N}_4\text{S}_3$ : C, 74.97; H, 4.38; N, 7.60%. Found: C, 74.77; H, 4.42; N, 7.52%.

**Compound 12.** The procedure for the synthesis of compound 11 was repeated except that 5,5'-bis(trimethylstannyl)-2,2'-bithiophene (0.24 g, 0.49 mmol) was used instead of 2,5-bis(trimethylstannyl)thiophene (0.20 g, 0.49 mmol). Yield: 0.27 g (68%). mp > 250 °C. Main FT-IR absorptions (KBr pellets,  $\text{cm}^{-1}$ ): 3442 (b), 1589 (s), 1487 (s), 1408 (m), 1322 (m), 1275 (s), 1110 (m), 756 (m), 694 (s).  $^1\text{H}$  NMR (500 MHz,  $\text{CDCl}_3$ ):  $\delta$  7.86 (s, 2H, thiazolyl), 7.78 (d, 4H,  $J = 7.6$  Hz, triphenylamino), 7.32–7.29 (t, 8H, triphenylamino), 7.15 (d, 8H,  $J = 8.2$  Hz, triphenylamino), 7.12 (d, 4H,  $J = 4.2$  Hz, thienyl), 7.10–7.07 (t, 8H, triphenylamino).  $^{13}\text{C}$  NMR (125 MHz,  $\text{CDCl}_3$ ):  $\delta$  167.3, 149.9, 147.0, 140.7, 132.1, 132.0, 128.5, 127.5, 125.7, 125.3, 124.0, 122.0. EI-TOF-MS ( $m/z$ ): calcd for  $[\text{C}_{50}\text{H}_{34}\text{N}_4\text{S}_4]^+$  818.2 (100.0), 819.2 (57.7), 820.2 (18.1), found 818.1 (100.0), 819.1 (63.5), 820.1 (8.9). Anal. calcd for  $\text{C}_{50}\text{H}_{34}\text{N}_4\text{S}_4$ : C, 73.32; H, 4.18; N, 6.84%. Found: C, 73.08; H, 4.24; N, 6.78%.

## ■ ASSOCIATED CONTENT

### ■ Supporting Information

Tables of selected bond lengths and angles and intermolecular hydrogen bonds; figures of  $\pi$ - $\pi$  stacking interactions;  $^1\text{H}$ ,  $^{13}\text{C}$ ,  $^1\text{H}$ - $^1\text{H}$  COSY NMR and EI-TOF-MS spectra; DFT computational details; and electrochemistry diagrams for related compounds. CCDC numbers 946825–946830 for compounds 2, 3, 5, and 7–9. This material is available free of charge via the Internet at <http://pubs.acs.org>.

## ■ AUTHOR INFORMATION

### Corresponding Author

\*E-mail: [whuang@nju.edu.cn](mailto:whuang@nju.edu.cn).

### Notes

The authors declare no competing financial interest.

## ■ ACKNOWLEDGMENTS

This work was financially supported by the Major State Basic Research Development Programs (Nos. 2013CB922101 and 2011CB933300), the National Natural Science Foundation of China (Nos. 21171088 and 21021062), and the Qing Lan Project.

## ■ REFERENCES

- (1) (a) Otsubo, T.; Aso, Y.; Takimiya, K. *J. Mater. Chem.* **2002**, *12*, 2565–2575. (b) Bocstaller, M. R.; Mickiewicz, R. A.; Thomas, E. L. *Adv. Mater.* **2005**, *17*, 1331–1349. (c) Gonzalez-Rodriguez, D.; Schenning, A. P. H. *J. Chem. Mater.* **2011**, *23*, 310–325. (d) Beaujeu, P. M.; Frechet, J. M. J. *J. Am. Chem. Soc.* **2011**, *133*, 20009–20029. (e) Li, H.-G.; Choi, J.-Y.; Nakanishi, T. *Langmuir* **2013**, *29*, 5394–5406. (f) Mahuteau-Betzer, F.; Piguel, S. *Tetrahedron Lett.* **2013**, *54*, 3188–3193.
- (2) Selected examples: (a) Zhang, M.; Tsao, H. N.; Pisula, W.; Yang, C.; Mishra, A. K.; Mullen, K. *J. Am. Chem. Soc.* **2007**, *129*, 3472–3473. (b) Hou, J.-H.; Chen, H.-Y.; Zhang, S.-Q.; Li, G.; Yang, Y. *J. Am. Chem. Soc.* **2008**, *130*, 16144–16145. (c) Sonar, P.; Singh, S. P.; Leclere, P.; Surin, M.; Lazzaroni, R.; Lin, T.-T.; Dodabalapur, A.; Sellinger, A. *J. Mater. Chem.* **2009**, *19*, 3228–3237. (d) Neto, B. A. D.; Lapis, A. A. M.; Da Silva, E. N.; Dupont, J. *Eur. J. Org. Chem.* **2013**, 228–255.
- (3) Selected examples: (a) Perepichka, I. F.; Perepichka, D. F., Eds. *Handbook of Thiophene-Based Materials: Applications in Organic Electronics and Photonics*; John Wiley & Sons: New York, 2009. (b) Niimi, K.; Shinamura, S.; Osaka, I.; Miyazaki, E.; Takimiya, K. *J. Am. Chem. Soc.* **2011**, *133*, 8732–8739. (c) Tanaka, S.; Tanaka, D.; Tatsuta, G.; Murakami, K.; Tamba, S.; Sugie, A.; Mori, A. *Chem.—Eur. J.* **2013**, *19*, 1658–1665. (d) Cai, N.; Wang, Y.-L.; Xu, M.-F.; Fan, Y.; Li, R.-Z.; Zhang, M.; Wang, P. *Adv. Funct. Mater.* **2013**, *23*, 1846–1854.
- (4) Selected examples: (a) Boudreaux, P. L. T.; Wakim, S.; Blouin, N.; Simard, M.; Tessier, C.; Tao, Y.; Leclerc, M. *J. Am. Chem. Soc.* **2007**, *129*, 9125–9136. (b) Hahm, S. G.; Lee, T. J.; Kim, D. M.; Kwon, W.; Ko, Y.-G.; Michinobu, T.; Ree, M. *J. Phys. Chem. C* **2011**, *115*, 21954–21962. (c) Mutkins, K.; Chen, S. S. Y.; Pivrikas, A.; Aljada, M.; Burn, P. L.; Meredith, P.; Powell, B. J. *Poly. Chem.* **2013**, *4*, 916–925. (d) Huang, H.; Wang, Y.-X.; Pan, B.; Yang, X.; Wang, L.; Chen, J.-S.; Ma, D.-G.; Yang, C.-L. *Chem.—Eur. J.* **2013**, *19*, 1828–1834.
- (5) Selected examples: (a) Chevallier, F.; Mongin, F. *Chem. Soc. Rev.* **2008**, *37*, 596–609. (b) Donghi, D.; D'Alfonso, G.; Mauro, M.; Panigati, M.; Mercandelli, P.; Sironi, A.; Mussini, P.; D'Alfonso, L. *Inorg. Chem.* **2008**, *47*, 4243–4255. (c) Ortiz, R. P.; Casado, J.; Hernandez, V.; Navarrete, J. T. L.; Letizia, J. A.; Ratner, M. A.; Facchetti, A.; Marks, T. J. *Chem.—Eur. J.* **2009**, *15*, 5023–5039. (d) Achelle, S.; Ple, N.; Turck, A. *RSC Adv.* **2011**, *1*, 364–388. (e) Achelle, S.; Ple, N. *Curr. Org. Synth.* **2012**, *9*, 163–187. (f) Achelle, S.; Baudequin, C.; Ple, N. *Dyes Pigm.* **2013**, *98*, 575–600.
- (6) Selected examples: (a) Bhosale, Sh. V.; Bhosale, Si. V.; Kalyankar, M. B.; Langford, S. J. *Org. Lett.* **2009**, *11*, 5418–5421. (b) Tao, T.; Lei, Y.-H.; Peng, Y.-X.; Wang, Y.; Huang, W.; Chen, Z.-X.; You, X.-Z. *Cryst. Growth Des.* **2012**, *12*, 4580–4587. (c) Gu, C.-L.; Hu, W.-P.; Yao, J.-N.; Fu, H.-B. *Chem. Mater.* **2013**, *25*, 2178–2183. (d) Getmanenko, Y. A.; Polander, L. E.; Hwang, D. K.; Tiwari, S. P.; Galan, E.; Seifried, B. M.; Sandhu, B.; Barlow, S.; Timofeeva, T.; Kippelen, B.; Marder, S. R. *J. Org. Semicond.* **2013**, *1*, 7–15.
- (7) Selected examples: (a) Herrmann, A.; Weil, T.; Sinigersky, V.; Wiesler, U. M.; Vosch, T.; Hofkens, J.; De Schryver, F. C.; Mullen, K. *Chem.—Eur. J.* **2001**, *7*, 4844–4853. (b) Addicott, C.; Oesterling, I.; Yamamoto, T.; Mullen, K.; Stang, P. J. *J. Org. Chem.* **2005**, *70*, 797–801. (c) Shin, W. S.; Jeong, H. H.; Kim, M. K.; Jin, S. H.; Kim, M. R.; Lee, J. K.; Lee, J. W.; Gal, Y. S. *J. Mater. Chem.* **2006**, *16*, 384–390. (d) Kim, B. J.; Yu, H.; Oh, J. H.; Kang, M. S.; Cho, J. H. *J. Phys. Chem. C* **2013**, *117*, 10743–10749.
- (8) Selected examples: (a) Chan, S.-C.; Chan, M. C. W.; Wang, Y.; Che, C.-M.; Cheung, K.-K.; Zhu, N.-Y. *Chem.—Eur. J.* **2001**, *7*, 4180–4190. (b) Xiao, S.-Z.; Yi, T.; Zhou, Y.-F.; Zhao, Q.; Li, F.-Y.; Huang, C.-H. *Tetrahedron* **2006**, *62*, 10072–10078. (c) Engel, Y.; Dahan, A.; Rozenshine-Kemelmakher, E.; Gozin, M. *J. Org. Chem.* **2007**, *72*, 2318–2328. (d) Maggioni, D.; Fenili, F.; D'Alfonso, L.; Donghi, D.; Oanigati, M.; Zanoni, I.; Marzi, R.; Manfredi, A.; Ferruti, P.; D'Alfonso, G.; Ranucci, E. *Inorg. Chem.* **2012**, *51*, 12776–12788.

- (9) (a) Kulkarni, A. P.; Tonzola, C. J.; Babel, A.; Jenekhe, S. A. *Chem. Mater.* **2004**, *16*, 4556–4573. (b) Frere, P.; Skabara, P. J. *Chem. Soc. Rev.* **2005**, *34*, 69–98. (c) Anthony, J. E. *Chem. Rev.* **2006**, *106*, 5028–5048. (d) Murphy, A. R.; Frechet, J. M. J. *Chem. Rev.* **2007**, *107*, 1066–1096. (e) Davis, R.; Kumar, N. S. S.; Abraham, S.; Suresh, C. H.; Rath, N. P.; Tamaoki, N.; Das, S. J. *Phys. Chem. C* **2008**, *112*, 2137–2146. (f) Mas-Torrent, M.; Rovira, C. *Chem. Rev.* **2011**, *111*, 4833–4856. (g) Huong, V. T. T.; Nguyen, H. T.; Tai, T. B.; Nguyen, M. J. *Phys. Chem. C* **2013**, *117*, 10175–10184.
- (10) Job, A.; Wakamiya, A.; Kehr, G.; Erker, G.; Yamaguchi, S. *Org. Lett.* **2010**, *12*, 5470–5473.
- (11) (a) Wang, C.-L.; Dong, H.-L.; Li, H.-X.; Zhao, H.-P.; Meng, Q.; Hu, W.-P. *Cryst. Growth Des.* **2010**, *10*, 4155–4160. (b) Burke, K. B.; Shu, Y.; Kempainen, P.; Singh, B.; Bown, M.; Liaw, I. I.; Williamson, R. M.; Thomsen, L.; Dastoor, P.; Belcher, W.; Forsyth, C.; Winzenberg, K. N.; Collis, G. E. *Cryst. Growth Des.* **2012**, *12*, 725–731.
- (12) (a) Huang, W.; Masuda, G.; Maeda, S.; Tanaka, H.; Ogawa, T. *Chem.—Eur. J.* **2006**, *12*, 607–619. (b) Huang, W.; Tanaka, H.; Ogawa, T. *J. Phys. Chem. C* **2008**, *112*, 11513–11526. (c) Huang, W.; Masuda, G.; Maeda, S.; Tanaka, H.; Hino, T.; Ogawa, T. *Inorg. Chem.* **2008**, *47*, 468–480. (d) Huang, W.; Wang, L.; Tanaka, H.; Ogawa, T. *Eur. J. Inorg. Chem.* **2009**, 1321–1330. (e) Huang, W.; Tanaka, H.; Ogawa, T.; You, X.-Z. *Adv. Mater.* **2010**, *22*, 2753–2758. (f) Hu, B.; Fu, S.-J.; Xu, F.; Tao, T.; Zhu, H.-Y.; Cao, K.-S.; Huang, W.; You, X.-Z. *J. Org. Chem.* **2011**, *76*, 4444–4456. (g) Tao, T.; Peng, Y.-X.; Huang, W.; You, X.-Z. *J. Org. Chem.* **2013**, *78*, 2472–2481. (h) Tao, T.; Qian, H.-F.; Zhang, K.; Geng, J.; Huang, W. *Tetrahedron* **2013**, *69*, 7290–7299.
- (13) Selected examples: (a) Wang, S.; Zuo, J.-L.; Zhou, H.-C.; Choi, H. J.; Ke, Y.-X.; Long, J. R.; You, X.-Z. *Angew. Chem., Int. Ed.* **2004**, *43*, 5940–5943. (b) Casado, J.; Delgado, M. C. R.; Merchan, M. C. R.; Hernandez, V.; Navarrete, J. T. L.; Pappenfus, T. M.; Williams, N.; Stegner, W. J.; Johnson, J. C.; Edlund, B. A.; Janzen, D. E.; Mann, K. R.; Orduna, J.; Villacampa, B. *Chem.—Eur. J.* **2006**, *12*, 5458–5470. (c) Sartin, M. M.; Camerel, F.; Ziessel, R.; Bard, A. J. *J. Phys. Chem. C* **2008**, *112*, 10833–10841. (d) Fischer, G. M.; Jungst, C.; Isomaki-Krondahl, M.; Gauss, D.; Mollor, H. M.; Daltrozzo, E.; Zumbusch, A. *Chem. Commun.* **2010**, *46*, 5289–5291. (e) Aydin, A. E. *Tetrahedron: Asymmetry* **2013**, *24*, 444–448. (f) Rinehart, J. D.; Long, J. R. *Chem. Sci.* **2011**, *2*, 2078–2085. (g) Zhang, W.; Xiong, R.-G. *Chem. Rev.* **2012**, *112*, 1163–1195.
- (14) (a) Dondoni, A.; Marra, A. *Chem. Rev.* **2004**, *104*, 2557–2600. (b) Wu, Y.-Z.; Zhu, W.-H. *Chem. Soc. Rev.* **2013**, *42*, 2039–2058.
- (15) (a) Martin, T.; Verrier, C.; Hoarau, C.; Marsais, F. *Org. Lett.* **2008**, *10*, 2909–2912. (b) Theveau, L.; Verrier, C.; Lassalas, P.; Martin, T.; Dupas, G.; Querolle, O.; Hijfte, L. V.; Marsais, F.; Hoarau, C. *Chem.—Eur. J.* **2011**, *17*, 14450–14463. (c) Fu, X.-P.; Xuan, Q.-Q.; Liu, L.; Wang, D.; Chen, Y.-J.; Li, C.-J. *Tetrahedron* **2013**, *69*, 4436–4444.
- (16) (a) Gottumukkala, A. L.; Doucet, H. *Eur. J. Inorg. Chem.* **2007**, 3629–3632. (b) Besselièvre, F.; Mahuteau-Betzer, F.; Grierson, D. S.; Piquel, S. J. *Org. Chem.* **2008**, *73*, 3278–3280. (c) Verrier, C.; Martin, T.; Hoarau, C.; Marsais, F. *J. Org. Chem.* **2008**, *73*, 7383–7386. (d) Ding, Z.-H.; Yoshikai, N. *Synthesis* **2011**, *16*, 2561–2566.
- (17) (a) Alberico, D.; Scott, M. E.; Lautens, M. *Chem. Rev.* **2007**, *107*, 174–238. (b) Chen, X.; Engle, K. M.; Wang, D.-H.; Yu, J.-Q. *Angew. Chem., Int. Ed.* **2009**, *48*, 5094–5115. (c) Daugulis, O.; Do, H.-Q.; Shabashov, D. *Acc. Chem. Res.* **2009**, *42*, 1074–1086. (d) Roger, J.; Gottumukkala, A. L.; Doucet, H. *ChemCatChem* **2010**, *2*, 20–40.
- (18) (a) Wiosna, G.; Petkova, I.; Mudadu, M. S.; Thummel, R. P.; Waluk, J. *Chem. Phys. Lett.* **2004**, *400*, 379–383. (b) Yang, P.-J.; Chu, H.-C.; Chen, T.-C.; Lin, H.-C. *J. Mater. Chem.* **2012**, *22*, 12358–12368. (c) Liu, Q.-Q.; Geng, J.; Wang, X.-X.; Gu, K.-H.; Huang, W.; Zheng, Y.-X. *Polyhedron* **2013**, *59*, 52–57.
- (19) (a) Ibrahim, Y. A.; Al-Awadi, N. A.; Ibrahim, M. R. *Tetrahedron* **2004**, *60*, 9121–9130. (b) Zanitato, P.; Cerini, S. *Org. Biomol. Chem.* **2005**, *3*, 1508–1513. (c) Kawai, S.; Nakashima, T.; Atsumi, K.; Sakai, T.; Harigai, M.; Imamoto, Y.; Kamikubo, H.; Kataoka, M.; Kawai, T. *Chem. Mater.* **2007**, *19*, 3479–3483. (d) Sarma, M.; Chatterjee, T.; Ghanta, S.; Das, S. K. *J. Org. Chem.* **2012**, *77*, 432–444. (e) Umeyama, T.; Hirose, K.; Noda, K.; Matsushige, K.; Shishido, T.; Saarenmaa, H.; Tkachenko, N. V.; Lemmetyinen, H.; Ono, N.; Imahori, H. *J. Phys. Chem. C* **2013**, *117*, 10175–10184.
- (20) (a) Bruno, C.; Paolucci, F.; Marcaccio, M.; Benassi, R.; Fontanesi, C.; Mucci, A.; Parenti, F.; Preti, L.; Schenetti, L.; Vanossi, D. *J. Phys. Chem. B* **2010**, *114*, 8585–8592. (b) Ma, C.-Q.; Pisula, W.; Weber, C.; Feng, X.-L.; Mullen, K.; Bauerle, P. *Chem.—Eur. J.* **2011**, *17*, 1507–1518.
- (21) (a) Turbiez, M.; Frere, P.; Roncali, J. *J. Org. Chem.* **2003**, *68*, 5357–5360. (b) Araki, K.; Endo, H.; Masuda, G.; Ogawa, T. *Chem.—Eur. J.* **2004**, *10*, 3331–3340. (c) Collis, G. E.; Campbell, W. M.; Officer, D. L.; Burrell, A. K. *Org. Biomol. Chem.* **2005**, *3*, 2075–2084. (d) Hergue, N.; Frere, P. *Org. Biomol. Chem.* **2007**, *5*, 3442–3449. (e) Kuzuhara, D.; Mack, J.; Yamada, H.; Okujima, T.; Ono, N.; Kobayashi, N. *Chem.—Eur. J.* **2009**, *15*, 10060–10069. (f) Balandier, J. Y.; Quist, F.; Amato, C.; Bouzakroui, S.; Cornil, J.; Sergeev, S.; Geerts, Y. *Tetrahedron* **2010**, *66*, 9560–9572. (g) Lin, Y.-Z.; Cheng, P.; Liu, Y.; Shi, Q.-Q.; Hu, W.-P.; Li, Y.-F.; Zhan, X.-W. *Org. Electron.* **2012**, *13*, 673–680.
- (22) (a) Chao, C. C.; Leung, M. K.; Su, Y. O.; Chiu, K. Y.; Lin, T. H.; Shieh, S. J.; Lin, S. C. *J. Org. Chem.* **2005**, *70*, 4323–4331. (b) Li, C.; Yum, J. H.; Moon, S. J.; Herrmann, A.; Eickemeyer, F.; Pschirer, N. G.; Erk, P.; Schoneboom, J.; Mullen, K.; Gratzel, M.; Nazeeruddin, M. K. *ChemSusChem* **2008**, *1*, 615–618. (c) Li, C.; Liu, Z.; Schoneboom, J.; Eickemeyer, F.; Pschirer, N. G.; Erk, P.; Herrmann, A.; Mullen, K. *J. Mater. Chem.* **2009**, *19*, 5405–5415. (d) Mathew, S.; Imahori, H. *J. Mater. Chem.* **2011**, *21*, 7166–7174. (e) Keerthi, A.; Valiyaveetil, S. J. *Phys. Chem. B* **2012**, *116*, 4603–4614. (f) Keerthi, A.; Liu, Y.; Wang, Q.; Valiyaveetil, S. *Chem.—Eur. J.* **2012**, *18*, 11669–11676.
- (23) Frisch, M. J.; et al. *Gaussian 09*, revision C.01; Gaussian, Inc.: Wallingford, CT, 2010.
- (24) Marcus, R. A. *J. Chem. Phys.* **1956**, *24*, 966–978.
- (25) Janaki, N. L.; Priyanka, B.; Thomas, A.; Bhanuprakash, K. *J. Phys. Chem. C* **2012**, *116*, 22663–22674.